We are IntechOpen, the world's leading publisher of Open Access books Built by scientists, for scientists

4,800
Open access books available

122,000
International authors and editors

135M
Downloads

Our authors are among the

154
Countries delivered to

TOP 1%
most cited scientists

12.2%
Contributors from top 500 universities

CLARIVATE ANALYTICS BOOK CITATION INDEX INDEXED

WEB OF SCIENCE™

Selection of our books indexed in the Book Citation Index in Web of Science™ Core Collection (BKCI)

Interested in publishing with us?
Contact book.department@intechopen.com

Numbers displayed above are based on latest data collected.
For more information visit www.intechopen.com

Chapter 7

Non-Linearity in Structural Dynamics and Experimental Modal Analysis

Ulrich Fuellekrug

Additional information is available at the end of the chapter

http://dx.doi.org/10.5772/48812

1. Introduction

During the mechanical design and development of technical systems for power plants, in civil engineering, aerospace or mechanical engineering increasing demands are made concerning the performance, weight reduction and utilization of the material. The consequence is that the dynamical behaviour and the occurrence of vibrations of the load carrying parts, the so-called primary structures are becoming more and more important. It has to be avoided that undesired vibrations can disturb or even jeopardize the intended operation. Thus, the analysis of the dynamics and vibrations of structures is an important task. To perform dynamic analyses and to draw conclusions for possibly needed changes of the mechanical design several steps have to be carried out.

First, the dynamic analysis requires computational models which may be setup with the Finite Element Method (FEM) or other adequate techniques. Second, the computational models have to be validated because otherwise no reliable theoretical predictions are possible which can be used for optimizing the mechanical design. For the validation of the computational models it is required to perform experiments on components, prototypes or the structures themselves. In many cases the structures can be considered as linear and thus linear structural dynamics methods and approaches can be applied for modelling and validation. However, in some cases non-linear effects are important and have to be taken into account (Awrejcewicz & Krysko, 2008). If this is the case, it is not sufficient to include non-linearities only in the models. Also the experimental validation has to be able to identify, characterize and quantify non-linearities (Awrejcewicz, Krysko, Papkova, & Krysko, 2012), (Krysko, Awrejcewicz, Papkova, & Krysko, 2012), (Awrejcewicz, Krysko, Papkova, & Krysko, 2012).

Let us first consider the dynamic equations of structures with non-linearities, then take a look at experimental dynamic identification and modal analysis before we develop basic ideas for identifying non-linearities of structures.

2. Equations of motion for structures

Most large and complex technical structures, or at least large parts of them, can be considered as elastomechanical systems. That means, the dynamic behaviour and the vibration characteristics are determined by the quantity and distribution of masses, stiffness and damping. In principle, all of these structures are assembled by continuous parts. However, an analysis of continuous structures is only possible if the geometry is rather simple. Beams, plates and shells can be analysed by using ordinary or partial differential equations. However, the coupling of the basic elements, which are described by differential equations, becomes difficult and impossible due to complicated boundary conditions if the number of elements is high. Under practical considerations it is appropriate to discretize the structures. Discrete points have to be defined at all suitable locations and the dynamic motions are described by motions of these discrete points. If a computational analysis with e.g. the Finite Element Method (FEM) is performed the nodal points are such discrete points. If an experimental analysis is carried out, suitable points have to be defined. Here, it is essential to select all structural points which are required to describe the dynamic motions with sufficient accuracy. The displacements, velocities and accelerations of the selected discrete points can then be assembled in the vectors $\{u\}, \{\dot{u}\}$ and $\{\ddot{u}\}$, the so-called displacement, velocity and acceleration vectors.

The equations of motion can be setup with different methods. As most general method, *Hamilton's* principle of least action (Williams, 1996), (Szabo, 1956), (Landau & Lifschitz, 1976) can be utilized. *Hamilton's* principle states that the time integral

$$\Im = \int_{t_1}^{t_2} \left(L + W \right) dt, \tag{1}$$

which contains *Lagrange's* function L and the work of non-conservative forces W, reaches a stationary value for the actual dynamic motions of the structure. The meaning of *Hamilton's* principle is that from all possible dynamic motions between two fixed states at points in time t_1 and t_2 the actual dynamic motions are those which cause a stationary value of the time integral of Eq. (1). Thus, arbitrary variations of Eq. (1) have to vanish and this leads to a method for setting up equations of motion (Williams, 1996).

Lagrange's L function consists of the kinetic and potential energy of the structure and can be written as

$$L = E_{kin} - E_{pot}. \tag{2}$$

The work of non-conservative forces $\{F\}$ can be computed with the displacements at discrete points $\{u\}$ at two fixed states at points in time t_1 and t_2 to

$$W = \int_{\{u(t_1)\}}^{\{u(t_2)\}} \{F\}^T d\{u\}. \tag{3}$$

Let us now separate notionally the structure in a complete linear part and some non-linear elements. In this case the kinetic energy of the linear part can be written with the physical mass matrix $\left[M\right]$ and the velocities $\left\{\dot{u}\right\}$ as follows

$$E_{kin} = \frac{1}{2}\left\{\dot{u}\right\}^T \left[M\right]\left\{\dot{u}\right\}. \tag{4}$$

In a similar way the potential energy of the structure's linear part is given by the physical stiffness matrix $\left[K\right]$ and the elastic deformations $\left\{u\right\}$ to

$$E_{pot} = \frac{1}{2}\left\{u\right\}^T \left[K\right]\left\{u\right\}. \tag{5}$$

The work of the non-conservative forces consists firstly of the work of the external forces $\left\{F_{ext}\right\}$ and the related deformations $\left\{u\right\}$

$$W_{ext} = \left\{u\right\}^T \left\{F_{ext}\right\}. \tag{6}$$

The damping of the elastomechanical structure can be taken into account by assuming discrete dampers, separating notionally the damping elements from the structure and considering the damping forces as external forces. Following this, the work of the damping forces is given for the structure's linear part by the physical damping matrix $\left[C\right]$ and the velocities $\left\{\dot{u}\right\}$ to

$$W_c = -\left\{u\right\}^T \left[C\right]\left\{\dot{u}\right\}, \tag{7}$$

where the minus sign indicates that the damping forces act into the opposite direction of the related velocities.

At next, the non-linear part of the structure has to be taken into account. Here, all non-linear elements are considered as discrete elements, are notionally separated from the linear structure and it is assumed that the forces between the structure and the non-linear elements depend only from the deformations and velocities at the connection points

$$\left\{F_{nl}\right\} = \left\{F_{nl}\left(\left\{u\right\},\left\{\dot{u}\right\}\right)\right\}. \tag{8}$$

Thus, the non-linearities of the structure can be considered as the effect of external forces. Following this, the work of the non-linear forces is given by

$$W_{nl} = -\int_{\left\{u(t_1)\right\}}^{\left\{u(t_2)\right\}} \left\{F_{nl}\left(\left\{u\right\},\left\{\dot{u}\right\}\right)\right\} d\left\{u\right\} \tag{9}$$

where the minus sign indicates that the non-linear forces act into the opposite direction of the related deformations and velocities.

The work of the non-conservative forces can now be written as

$$W = W_{ext} + W_c + W_{nl} = \{u\}^T \{F_{ext}\} - \{u\}^T [C]\{\dot{u}\} - \int_{\{u(t_1)\}}^{\{u(t_2)\}} \left\{F_{nl}\left(\{u\},\{\dot{u}\}\right)\right\} d\{u\} . \tag{10}$$

The variation of Eq. (1)

$$\delta \Im = \delta \int_{t_1}^{t_2} (L + W) dt = \int_{t_1}^{t_2} \left(\delta E_{kin} - \delta E_{pot} + \delta W\right) dt = 0 \tag{11}$$

leads with Eqs. (4), (5) and (10) to

$$[M]\{\ddot{u}\} + [C]\{\dot{u}\} + [K]\{u\} + \left\{F_{nl}\left(\{u\},\{\dot{u}\}\right)\right\} = \{F\}, \tag{12}$$

which is the well-known basic equation of linear structural dynamics extended by a term accounting for non-linearities.

3. Dynamic identification and modal analysis

With the purpose to validate analytical models of complex technical structures it is required to perform measurements on components or prototypes and to identify the dynamic properties. The most important dynamic properties are the modal parameters. Their identification is the essential goal of experimental modal analysis (Maia & Silva, 1997), (Ewins, 2000).

3.1. Modal parameters

To explain the basic ideas, let us first assume that the structure undergoing a modal identification test is linear and that the damping matrix is proportional to the mass and stiffness matrix. In this case Eq. (12) simplifies to

$$[M]\{\ddot{u}\} + [C]\{\dot{u}\} + [K]\{u\} = \{F\}, \tag{13}$$

where it is assumed

$$[C] = \beta_1 [M] + \beta_2 [K] . \tag{14}$$

The eigenvalues und eigenvectors of the undamped structure are determined by the eigenvalue problem

$$\left(\omega_{0r}^2 [M] + [K]\right)\{\phi\}_r = \{0\} \tag{15}$$

and are of great practical importance. The values ω_{0r} are the so-called eigenfrequencies and $\{\phi\}_r$ are the eigenvectors of the undamped structure. A fundamental property of the eigenvectors $\{\phi\}_r$ is the fact that the matrix of eigenvectors, the so-called modal matrix, diagonalises the mass and stiffness matrices

$$\left[\phi\right]^T\left[M\right]\left[\phi\right]=\begin{bmatrix}\{\phi\}_1^T\\ \{\phi\}_2^T\\ \vdots\\ \{\phi\}_n^T\end{bmatrix}\left[M\right]\begin{bmatrix}\{\phi\}_1 & \{\phi\}_2 & \cdots & \{\phi\}_n\end{bmatrix}=\begin{bmatrix}m_1 & 0 & 0 & 0\\ 0 & m_2 & 0 & 0\\ 0 & 0 & \ddots & 0\\ 0 & 0 & 0 & m_n\end{bmatrix}, \tag{16}$$

$$\left[\phi\right]^T\left[K\right]\left[\phi\right]=\begin{bmatrix}\{\phi\}_1^T\\ \{\phi\}_2^T\\ \vdots\\ \{\phi\}_n^T\end{bmatrix}\left[K\right]\begin{bmatrix}\{\phi\}_1 & \{\phi\}_2 & \cdots & \{\phi\}_n\end{bmatrix}=\begin{bmatrix}k_1 & 0 & 0 & 0\\ 0 & k_2 & 0 & 0\\ 0 & 0 & \ddots & 0\\ 0 & 0 & 0 & k_n\end{bmatrix}. \tag{17}$$

The terms $m_1, m_2, \ldots, m_n$ are the so-called modal mass

$$m_r=\{\phi\}_r^T\left[M\right]\{\phi\}_r, \tag{18}$$

and in analogy, the terms $k_1, k_2, \ldots, k_n$ are the so-called modal stiffness

$$k_r=\{\phi\}_r^T\left[K\right]\{\phi\}_r. \tag{19}$$

In addition it is valid

$$\omega_{0r}=\sqrt{\frac{k_r}{m_r}}, \tag{20}$$

$$\zeta_r=\frac{c_r}{2\sqrt{k_r m_r}}, \tag{21}$$

where

$$c_r=\{\phi\}_r^T\left[C\right]\{\phi\}_r=\{\phi\}_r^T\left(\gamma_1\left[M\right]+\gamma_2\left[K\right]\right)\{\phi\}_r. \tag{22}$$

and

$$\omega_r=\omega_{0r}\sqrt{1-\zeta_r^2}. \tag{23}$$

Using the above modal parameters it can be shown that the dynamic responses of a structure (13) due to an impulse or a release from any initial condition are

$$\{u(t)\}=\sum_{r=1}^{n}\left(A_r\sin\omega_r t+B_r\cos\omega_r t\right)e^{-\zeta_r\omega_r t}\{\phi\}_r. \tag{24}$$

This equation reveals that the free decay vibrations are determined by a superposition of eigenvectors with damped harmonic vibrations at the respective eigenfrequencies. The contribution of each eigenvector depends on A_r and B_r, i.e. the initial conditions at time $t = 0$. The time history of the vibrations is determined by the eigenfrequency ω_r for the harmonic part and by the modal damping value ζ_r as well as the eigenfrequency ω_r for the decay part.

Also it can be shown that the steady state dynamic responses of a structure to a harmonic excitation with frequency ω

$$\left\{F\left(t\right)\right\} = \left\{\hat{F}\right\} e^{i\omega t} \tag{25}$$

is

$$\left\{u\left(t\right)\right\} = \left\{\hat{u}\right\} e^{i\omega t} = \sum_{r=1}^{n} \left\{\phi\right\}_r \frac{\left\{\phi\right\}_r^T \left\{\hat{F}\right\}}{m_r\left(\omega_{0r}^2 - \omega^2 + i2\zeta_r\omega_{0r}\omega\right)} e^{i\omega t}. \tag{26}$$

This equation shows that the steady state harmonic vibrations are defined by a superposition of eigenvectors with frequency dependent amplification or attenuation factors. The contribution of each eigenvector depends on the so-called modal force $\left\{\phi\right\}_r^T \left\{\hat{F}\right\}$, the modal mass m_r and the relationship of the excitation frequency ω to the respective eigenfrequency ω_{0r}. Near the resonance frequencies, where ω approaches ω_{0r}, i.e. $\omega \approx \omega_{0r}$, the modal damping ζ_r becomes important and limits the vibration amplitudes to finite values.

Considering Eqs. (24) and (26) shows that the complete dynamic behaviour of a complex structure is determined by a set of modal parameters $\omega_{0r}, \left\{\phi\right\}_r, m_r, \zeta_r$. Thus, the experimental identification of these parameters is of great practical importance and allows a detailed insight into the dynamic behaviour.

3.2. Experimental modal analysis

Since the 1970s numerous methods for experimental modal analysis have been developed (Maia & Silva, 1997), (Ewins, 2000), (Fuellekrug, 1988). In addition to the classical Phase Resonance Method (PhRM) a large number of Phase Separation Techniques (PhST) operating in the time or frequency domain has been developed and can be applied nowadays as a matter of routine during modal identification tests.

For the practical performance of high quality modal identification tests several concerns have to be accounted for. First, in many cases several hundred sensors are required to achieve a sufficient resolution of the spatial motions of all structural parts. Second, the excitation requires several large exciters which have to be operated simultaneously in order to excite all vibration modes. Third, the results have to be of high quality and accuracy since they are used for the verification and validation of analytical models. Therefore it has to be

assured that all modes in the requested frequency range are identified and that the accuracy of the modal parameters is as high as possible.

All these demands lead to the fact that a highly sophisticated concept for the modal identification is required (Gloth, et al., 2001). During the modal identification testing of large complex structures also the possible non-linear behaviour has to be investigated. Usually, linear dynamic behaviour of the structure is assumed in the applied modal identification methods. However, in practice most of the investigated and tested structures exhibit some non-linear behaviour. Such non-linear behaviour can occur for example as a result of free play and different connection categories (e.g. welded, bolted) within joints or e.g. from hydraulic systems in control surfaces of aircraft.

4. Non-linear modal identification

The classical procedure for the modal identification is to perform normal-mode force appropriation with the Phase Resonance Method (PhRM). The structure is harmonically excited by means of an excitation force pattern appropriated to a single mode of vibration. However, the exclusive application of the Phase Resonance Method (PhRM) is time-consuming. Thus, an improved test concept is required which combines Phase Resonance Method (PhRM) with Phase Separation Techniques (PhST).

The core of such an optimized test concept applied e.g. to aircraft as Ground Vibrations Tests (GVT) is to combine consistently Phase Separation Techniques and the Phase Resonance Method with their particular advantages (Gloth, et al., 2001), see Figure 1. After the setup the GVT starts with the measurement of Frequency Response Functions (FRFs) in optimized exciter configurations. Second, the FRFs are analysed with Phase Separation Techniques. Hereafter the Phase Resonance Method is applied for selected vibration modes, e.g. for modes that indicate significant deviations from linearity, for modes known to be important for flutter calculations (if an aircraft is tested), or for modes which significantly differ from the prediction of the finite element analysis. Optimal exciter locations and amplitudes can be calculated from the already measured FRFs in order to accelerate the time-consuming appropriation of the force vector. The calculated force vector is applied and the corresponding eigenvector is tuned. Once a mode is identified, the classical methods for identifying modal damping and modal mass are applied. Also, a linearity check by simply increasing the excitation level is performed. During this linearity check, a possible change of the modal parameters with the force level can be investigated, see (Goege, Sinapius, Fuellekrug, & Link, 2005).

The identified eigenvectors are compared with the prediction of the finite element model and by themselves during the measurement in order to check the completeness of the data and its reliability. Multiply identified modes are sorted out. Additional exciter configurations have to be used and certain frequency ranges need to be investigated if not all expected modes are experimentally identified or if the quality of the results is not sufficient.

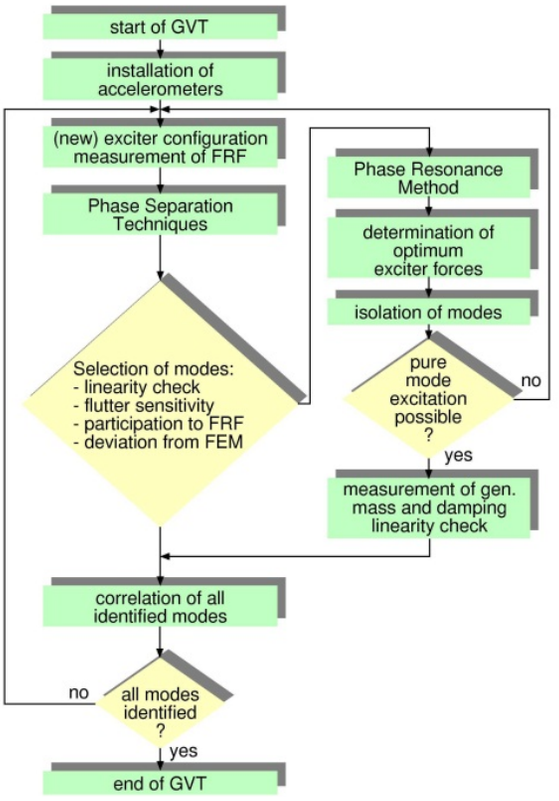

Figure 1. Test concept for modal identification of complex structures in a Ground Vibration Test (GVT)

4.1. Detection and identification of non-linearities

The above test concept allows the identification of non-linearities if some conditions are fulfilled: The response to harmonic excitation should be dominated by the excitation frequency and the mode shapes of the associated linear system should remain nearly unchanged at different force levels.

In order to characterize the non-linearities of a large complex structure, it is first required to detect the non-linearities. This can be done by simply increasing the force level. However, more detailed investigations are beneficial. The book (Worden & Tomlinson, 2001) gives a broad survey of non-linearities in structural dynamics. The detection, identification and modeling is described in great detail. Numerous suitable methods are presented and elucidated. The article (Gloth & Goege) proposes some methods for the fast detection of non-linearities within the described advanced modal survey test concept.

The step following the detection is the identification of the non-linearities. For complex lightly damped structures with weak non-linearities, the mode shapes can be divided into different groups as shown in (Wright, Platten, Cooper, & Sarmast, 2001):

- Linear proportionally damped modes, which are well separated in frequency.
- Linear proportionally damped modes, which are very close or identical in frequency.
- Linear non-proportionally damped modes, which are usually fairly close in frequency (significant damping coupling)

- Uncoupled modes, which are influenced by non-linear effects.
- Coupled modes, which are influenced by non-linear effects.

Most of the modes of real structures behave linear so that an identification using the classical linear methods and the test concept described above is still possible. Nevertheless, some modes show significant non-linear behaviour, which makes it impossible to adopt linear theory. A solution to this problem is a non-linear identification which can be based on the Masri-Caughey approach (Masri & Caughey, 1979), the force-state mapping (Crawley & Aubert, 1986) and a variant of it (Al_Hadid & Wright, 1989). The idea and basics of the non-linear resonant decay method (NLRDM) (Wright, Platten, Cooper, & Sarmast, 2001), (Platten, Wright, Cooper, & Sarmast, 2002), (Wrigth, Platten, Cooper, & Sarmast, 2003), (Platten, Wrigth, Worden, Cooper, & Dimitriadis, 2005), (Platten, Wrigth, Dimitriadis, & Cooper, 2009) appear to be an appropriated method for applying it to large and complex structures.

4.2. Basic equations for non-linear modal identification

In this section the theoretical background of the non-linear analysis of structures is outlined. The basic equations are established and a way for the modal identification in case of single non-linear modes and coupled non-linear modes is described.

The equations of motion for an elastomechanical system with linear and non-linear restoring forces are given according to Eq. (12) by

$$\left[M\right]\left\{\ddot{u}\right\}+\left[C\right]\left\{\dot{u}\right\}+\left[K\right]\left\{u\right\}+\left\{F_{nl}\left(\left\{u\right\},\left\{\dot{u}\right\}\right)\right\}=\left\{F_{ext}\right\}, \tag{27}$$

where, as above, $\left[M\right]$, $\left[C\right]$ and $\left[K\right]$ are the mass, damping and stiffness matrices, and $\left\{\ddot{u}\right\}$, $\left\{\dot{u}\right\}$ and $\left\{u\right\}$ are the vectors of physical displacements, velocities and accelerations. The non-linear restoring forces are given by $\left\{F_{nl}\left(\left\{u\right\},\left\{\dot{u}\right\}\right)\right\}$, and $\left\{F_{ext}\right\}$ is the vector of the external excitation forces.

The equations of motion Eq. (27) can be transformed from physical to modal space by using the modal matrix $\left[\phi\right]$ of the associated linear undamped system

$$\left\{u\left(t\right)\right\}=\sum_{r=1}^{n}\left\{\phi\right\}_{r}q_{r}(t)=\left[\phi\right]\left\{q(t)\right\} \tag{28}$$

where $\left\{q(t)\right\}$ is the vector of (generalized) modal coordinates, which represent modal degrees of freedom (DoF). Substituting the modal expansion of Eq. (28) into the equations of motion and pre-multiplying by the transposed of the modal matrix $\left[\phi\right]^{T}$ yields

$$\left[\phi\right]^{T}\left[M\right]\left[\phi\right]\left\{\ddot{q}\right\}+\left[\phi\right]^{T}\left[C\right]\left[\phi\right]\left\{\dot{q}\right\}+\left[\phi\right]^{T}\left[K\right]\left[\phi\right]\left\{q\right\}+\left[\phi\right]^{T}\left\{F_{nl}\left(\left\{u\right\},\left\{\dot{u}\right\}\right)\right\}=\left[\phi\right]^{T}\left\{F_{ext}\right\}. \tag{29}$$

This equation can be rewritten as

$$\left[m\right]\left\{\ddot{q}\right\}+\left[c\right]\left\{\dot{q}\right\}+\left[k\right]\left\{q\right\}+\left\{\delta\right\}=\left\{f_{ext}\right\}, \tag{30}$$

where $\left[m\right]$, $\left[c\right]$ and $\left[k\right]$ are the (generalized) modal mass, damping and stiffness matrices. The modal mass and stiffness matrices $\left[m\right]$, $\left[k\right]$ are diagonal since the real normal modes $\left\{\phi\right\}_r$ of the associated undamped system are orthogonal with respect to the physical mass and stiffness matrices $\left[M\right]$ and $\left[K\right]$. In case of so-called proportional damping also the modal damping matrix $\left[c\right]$ is diagonal. $\left\{\delta(t)\right\}$ is the vector of modal non-linear restoring forces, which includes stiffness and damping non-linearities, and $\left\{f_{ext}(t)\right\}$ is the vector of (generalized) modal excitation forces.

If the damping is proportional Eq. (30) simplifies to

$$m_r\ddot{q}_r+c_r\dot{q}_r+k_rq_r+\delta_r=f_r, \quad r=1,2,\ldots,n. \tag{31}$$

In case of $\delta_r(t)\equiv 0$, the dynamic equation for mode r is in the form of a single degree of freedom system. When the Phase Resonance Method according to the above described test concept is used, the excitation forces are appropriated to the specific mode and the whole structure vibrates in the linear case as a single DoF system. However, if non-linearities are present the modal DoF r may be coupled with other modal DoF. This is because the vector of the non-linear modal restoring forces $\left\{\delta(t)\right\}$ is, according to Eqs. (30) and (29), a function of all physical displacements and velocities

$$\left\{\delta(t)\right\}=\left[\phi\right]^T\left\{F_{nl}\left(\left\{u\right\},\left\{\dot{u}\right\}\right)\right\}. \tag{32}$$

And thus, in the general case, the non-linear modal restoring forces $\delta_r(t)$ can be a function of all modal coordinates

$$\delta_r=\delta_r(q_1,q_2,\ldots,q_n;\dot{q}_1,\dot{q}_2,\ldots,\dot{q}_n). \tag{33}$$

The basic idea of the non-linear modal identification is to use time domain data of the modal DoF and to perform a so-called direct parameter estimation (DPE) in the modal space (Worden & Tomlinson, 2001) as well as to apply ideas of the non-linear resonant decay method (NLRDM) (Wright, Platten, Cooper, & Sarmast, 2001), (Platten, Wright, Cooper, & Sarmast, 2002), (Wrigth, Platten, Cooper, & Sarmast, 2003), (Platten, Wrigth, Worden, Cooper, & Dimitriadis, 2005), (Platten, Wrigth, Dimitriadis, & Cooper, 2009).

When the excitation forces are appropriated the whole structure vibrates in the linear case as a single DoF system. Thus, the analysis in modal space offers an effective way of identifying the non-linear damping and stiffness properties. Such a non-linear identification requires the previous identification of the linear modal parameters mass m_r, damping c_r and stiffness k_r. Also, it is required to determine the time histories of the modal coordinates $q_r(t)$ and the modal forces $f_r(t)$.

The rearrangement of Eq. (31) delivers

$$\delta_r(t)=-m_r\ddot{q}_r(t)-c_r\dot{q}_r(t)-k_rq_r(t)+f_r(t). \tag{34}$$

Here, m_r, c_r and k_r are experimentally identified e.g. from vector polar plot curve fit, evaluation of real part slopes or from the complex power method, see (Niedbal & Klusowski, 1989). The modal coordinate $\ddot{q}_r(t)$ is calculated from the physical acceleration responses $\{\ddot{u}(t)\}$ and the modal matrix $[\phi]$ by solving Eq. (28) e.g. with least squares:

$$\{\ddot{q}(t)\} = \left([\phi]^T [\phi]^{-1}\right)[\phi]^T \{\ddot{u}(t)\}. \tag{35}$$

$[\phi]$ in Eq. (35) represents the experimental modal matrix. This modal matrix contains the eigenvectors in the frequency band of interest, which were previously determined from linear modal analysis. If significant modal responses for other than the investigated mode of vibration are observable, coupling terms between the investigated modes and other modes exist.

The modal velocities $\dot{q}_r(t)$ and modal displacement responses $\ddot{q}_r(t)$ of the mode can be obtained by an integration of the modal acceleration responses. Prior to the integration, a band-pass filtering of the data is required in order to avoid a drift of the time domain signals. The modal excitation force $f_r(t)$ is calculated from measured eigenvectors and excitation forces according to

$$f_r(t) = \{\phi\}_r^T \{F(t)\}. \tag{36}$$

With the purpose of identifying the non-linear parameters it is required to use an analytical expression which is able to describe the non-linear behaviour. If the modal DoF r is non-linear in the stiffness and depends only on the modal coordinate $q_r(t)$, a polynomial function like

$$\delta_r(t) = \alpha_1 q_r(t) + \alpha_3 q_r^3(t) + \alpha_5 q_r^5(t) + \ldots \tag{37}$$

can be used. The coefficient α_1 describes the linear part of the stiffness and α_3, α_5,. characterize the cubic and higher polynomial parts of the stiffness.
The coefficients α_i of the function can be computed by writing Eq. (37) for several time steps t_j

$$\begin{Bmatrix} \delta_r(t_1) \\ \delta_r(t_2) \\ \vdots \\ \delta_r(t_\ell) \end{Bmatrix} = \begin{bmatrix} q_r(t_1) & q_r^3(t_1) & q_r^5(t_1) & \cdots \\ q_r(t_2) & q_r^3(t_2) & q_r^5(t_2) & \cdots \\ \vdots & \vdots & \vdots & \cdots \\ q_r(t_\ell) & q_r^3(t_\ell) & q_r^5(t_\ell) & \cdots \end{bmatrix} \begin{Bmatrix} \alpha_1 \\ \alpha_3 \\ \alpha_5 \\ \vdots \end{Bmatrix}. \tag{38}$$

The vector on the left hand side of the equation can be computed from Eq. (34) by inserting values for the modal parameters, m_r, c_r, k_r and time domain data at time steps t_j with $j = 1,2,\ldots,\ell$ of the modal coordinates $\ddot{q}_r(t_j), \dot{q}_r(t_j), q_r(t_j)$, and the modal force $f_r(t_j)$. The matrix on the right hand side is formed by time domain data of the modal coordinate $q_r(t_j)$.

The solution of Eq. (38) with least squares or any other appropriate method delivers the coefficients $\alpha_1, \alpha_3, \alpha_5, \ldots$. Care is needed for the appropriate number of time steps in Eq. (38) because too few or too many time steps can cause problems.

The quality of the non-linear identification can be checked by comparing the restoring force $\delta_r(t)$ of Eq. (34), which is based on measured data, and the recalculated restoring force, which is computed from Eq. (37) with the identified coefficients α_i. However, in cases of weak non-linearities (small non-linear restoring forces) the deviations may be high, although the agreement for the modal coordinates is very good. For this reason it is better to compare the modal accelerations of the measurement $\ddot{q}_r(t)$ with the recalculated modal accelerations $\ddot{\tilde{q}}_r(t)$, which are computed from the rearranged Eq. (34)

$$\ddot{q}_r(t) = \frac{1}{m_r}\left(f_r(t) - c_r\dot{q}_r(t) - k_r q_r(t) - \delta_r(t)\right), \tag{39}$$

where $\delta_r(t)$ is computed from Eq. (37). A qualitative comparison can be performed by visualizing the time histories of $\ddot{q}_r(t)$ and $\ddot{\tilde{q}}_r(t)$. In addition, a quantitative comparison can be obtained by the root mean square (RMS) values of the measured acceleration signal and the deviation between measured and recalculated signals.

4.3. Single mode identification

If the non-linearity in the modal DoF r is solely caused by displacements $q_r(t)$ and velocities $\dot{q}_r(t)$ of the same DoF r , the problem of non-linear identification is reduced to a single DoF problem.

To model stiffness non-linearities a polynomial with even and odd powers of the displacements $q_r(t)$ can be used

$$\delta_{k,r}(t) = \sum_{i=0}^{i_{\max}} \alpha_i {q_r}^i(t). \tag{40}$$

The involvement of terms with even powers in Eq. (40) allows for possible non-symmetric characteristics of the overall restoring force. If only terms with odd powers were employed, the overall restoring force would be completely anti-symmetric. Of course, the number of terms i and the associated coefficients α_i determine whether the overall force $\delta_{k,r}(t)$ always acts into the opposite direction of the respective displacements and has really the physical meaning of a restoring force.

In a quite similar way, the damping non-linearities can be modelled by the function

$$\delta_{c,r}(t) = \sum_{i=0}^{i_{\max}} \gamma_i {\dot{q}_r}^i(t). \tag{41}$$

Here as well, the involvement of terms with even powers in Eq. (41) allows for possible non-symmetric characteristics of the restoring forces. If only terms with odd powers would be employed, the overall restoring force would be completely anti-symmetric.

If stiffness and damping non-linearities occur together the functions of Eqs. (40) and (41) can be combined. In some cases it may also be appropriate to use mixed terms with displacements and velocities.

By modelling the non-linearities with functions of Eq. (40), Eq. (41) or an appropriate combination the non-linear identification is reduced to the estimation of the coefficients α_i and γ_i. The computation of the coefficients is in all cases based on an equation like Eq. (38).

The article (Goege, Fuellekrug, Sinapius, Link, & Gaul, 2005) describes in detail the identification of the non-linear parameters for a single mode of vibration. In addition, the paper shows a way of characterizing the identified non-linearities. The Harmonic Balance is used, and on the basis of the identified non-linear parameters α_i and γ_i the dependency of eigenfrequency ω_r and damping ζ_r versus the excitation level can be calculated and visualised in graphs, the so-called modal characterizing functions.

4.4. Coupled mode identification

In the case of coupled modes the function of Eq. (40) has to be extended by the contribution of other modal coordinates $q_s(t)$. If two modes r and s are coupled with respect to the stiffness, the polynomial function

$$\delta_{k,r}(t) = \sum_{i=0}^{i_{\max}} \sum_{j=0}^{j_{\max}} \alpha_{ij} {q_r}^i(t) {q_s}^j(t) \tag{42}$$

can be used. As above, the involvement of terms with even powers in Eq. (42) allows for possible non-symmetric characteristics of the restoring forces.

To model damping non-linearities the polynomial function

$$\delta_{c,r}(t) = \sum_{i=0}^{i_{\max}} \sum_{j=0}^{j_{\max}} \gamma_{ij} {\dot{q}_r}^i(t) {\dot{q}_s}^j(t) \tag{43}$$

can be used. For more general cases the functions of Eqs. (42) and (43) can be combined. In some cases it may also be appropriate to use mixed terms with displacements and velocities. If three or more modes are non-linearly coupled the functions of Eqs. (42) and (43) can be extended accordingly. Also, the identification is not generally restricted to polynomial functions. Any other function may be used where it is appropriate. The important fact is that the function has to contain parameter coefficients, which can be computed from measured data by using a suitable identification equation.

The estimation of the coefficients of the functions in Eq. (42) or Eq. (43) always leads to the solution of an over-determined set of linear equations like

$$\{\Delta\} = [Q]\{\alpha\}, \tag{44}$$

where $\{\Delta\}$ contains the values of the non-linear restoring forces $\delta(t)$ at discrete time steps (computed according to Eq. (34)), $[Q]$ is comprised by time domain data of the modal coordinates $q_r(t), \dot{q}_r(t), q_s(t), \dot{q}_s(t)$ and vector $\{\alpha\}$ is assembled by the unknown coefficients α_{ij}, γ_{ij}. The solution of Eq. (44) can be obtained by using least squares. However, also other appropriate parameter estimation methods can be applied.

4.5. Summarization of steps for non-linear modal identification

The steps for performing a non-linear modal identification according to the above theory can be summarized as follows:

- Identify the linear modal characteristics of the tested structure with the Phase Resonance Method or Phase Separation Techniques.
- Detect the modes that behave non-linear.
- Excite the non-linear modes with appropriated exciter forces at different force levels and use harmonic or sine sweep excitation. Measure time domain signals of forced vibrations alone, or signals of forced and free decay vibrations.
- Compute the participation of the modal coordinates according to Eq. (35) and check if modes are coupled.
- Perform single mode non-linear identification for the uncoupled modes.
- Perform coupled non-linear mode identification for the coupled modes.
- Check the quality of the identification by comparing the measured and recalculated modal signals.

5. Illustrative analytical example

In this section the non-linear identification is applied to an analytical vibration system with 3 DoF. The purpose is to illustrate the principles of and to demonstrate the applicability.

The vibration system is shown in Figure 2. The non-linearity consists of a non-linear spring with a cubic characteristic ($F_{nl} = k_{nolin} \cdot u_2^3$). The non-linear spring is attached parallel to the medial spring k_2. The eigenfrequencies of the associated linear undamped system are located at *2.845 Hz, 3.774 Hz* and *8.954 Hz*. The modal matrix of the associated linear undamped vibration system is

$$[\phi] = \begin{bmatrix} \{\phi\}_1 & \{\phi\}_2 & \{\phi\}_3 \end{bmatrix} = \begin{bmatrix} 1 & -1 & -0.216 \\ 0.432 & 0 & 1 \\ 1 & 1 & -0.216 \end{bmatrix}, \tag{45}$$

where the columns of the modal matrix are the eigenvectors $\{\phi\}_r, r = 1,2,3$ with components at the 3 masses m_1, m_2, m_3. Due to the position of the non-linear spring, only modes 1 and 3 behave non-linear while mode 2 is completely linear. The reason is that mode 2 has no deformation at the attachment point of the non-linear spring k_{nolin}.

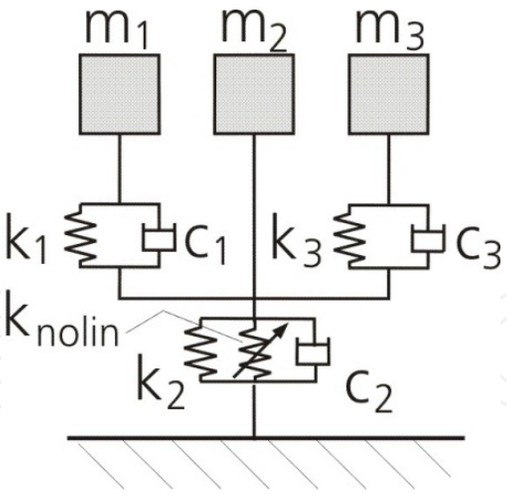

Figure 2. Vibration system with 3 Dof

For the simulation of 'measured' data the vibration system is excited with two single forces at mass 2 and mass 3. As excitation signal a sine sweep is used, which runs in *10 s* linearly from *2 Hz* to *12 Hz*.

For the non-linear analysis the *10 s* of the sine sweep excitation and *10 s* of the following free decay vibrations are used. The time domain integration of the 'measured' acceleration signals is realized by applying a digital band-pass filter to the accelerations and by integrating them once. The resulting velocities are also digitally band-pass filtered and then integrated to obtain displacements. Thus, no drift occurs during time domain integration. The force signals are also digitally high-pass filtered twice with the purpose to retain the correct phase relationship between the input and the output of the system.

Figure 3 shows the structural displacement responses following the above sine sweep excitation. *20 s* of the time histories of the modal coordinates $q_1(t)$, $q_2(t)$ and $q_3(t)$ are displayed. Figure 4 shows the mode participation of the modal coordinates as scaled root

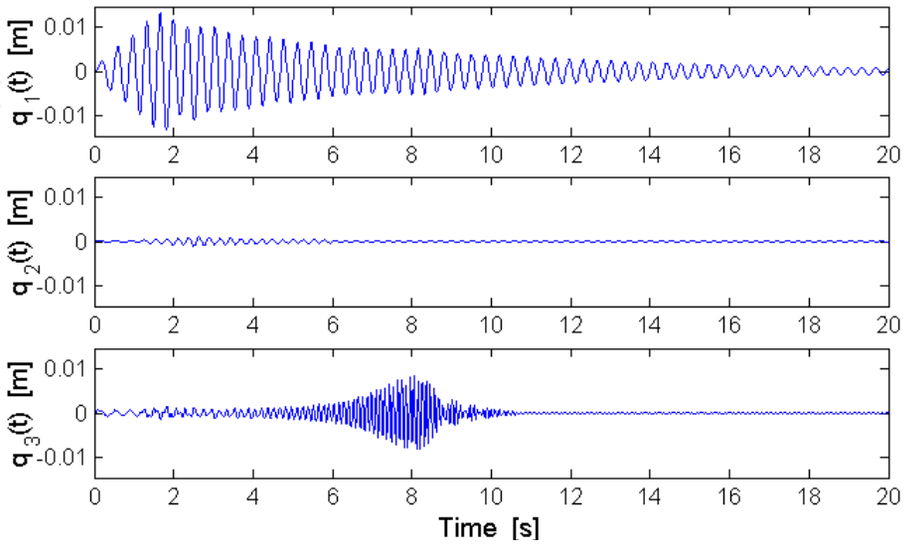

Figure 3. Time histories of the modal displacements

mean square (RMS) values. From the figures it can be seen that the above sine sweep excites clearly the modal DoF *1* and *3*, whereas DoF *2* responds only very weakly.

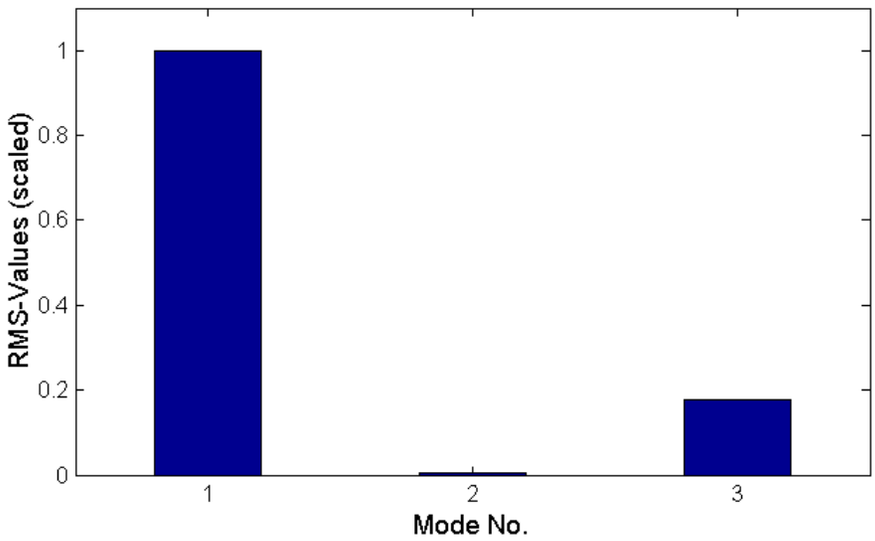

Figure 4. Mode participation

With the purpose to investigate the influence of measurement noise and errors in the data, a random signal with an RMS-value of *5 %* is added to the clean signals of excitation forces and responses prior to the non-linear identification. For the modal parameters m_r, c_r and k_r which are required for the computation of the non-linear restoring forces $\delta_r(t)$ according to Eq. (34), the correct values are used. Also, for the eigenvectors $\{\phi\}_r$ the correct data are used. A careful modal analysis at an appropriate excitation level should be able to deliver such accurate data of the underlying linear system.

In the following the simulated *20 s* time histories of $q_1(t)$, $q_2(t)$ and $q_3(t)$ are used for the non-linear modal identification. First, single mode identification on a trial basis is performed. The polynomial function of Eq. (40) with $i_{\max}$ increasing from *1* to *5* is employed. The result is always the same: the deviations between the 'measured' and recalculated signals remain high. Also, it shows that there are effects which cannot be accounted for with single mode non-linear identification. Figure 5 shows as an example the measured and recalculated restoring force of the modal DoF $r=1$ for $i_{\max}=5$. By the way, it is interesting that the usage of too much coefficients α_i causes no problems. The apparently unnecessary coefficients are computed to *0*.

Since the single mode non-linear identification is not sufficient, as next step coupled mode identification is performed. For the coupled mode identification the polynomial function of Eq. (42) is used. The number of terms is increased from $i_{\max}=j_{\max}=1$ to $i_{\max}=j_{\max}=3$. The deviations between the 'measured' and recalculated signals disappear completely for $i_{\max}=j_{\max}=3$ and if the clean signals (without the additional random noise) are utilized. Again, it shows that the usage of too many coefficients α_i causes no problems. The apparently unnecessary coefficients are computed to *0*. The analysis of noisy signals leads to deviations. However, the deviations are not much higher than the noise itself. E.g. in the

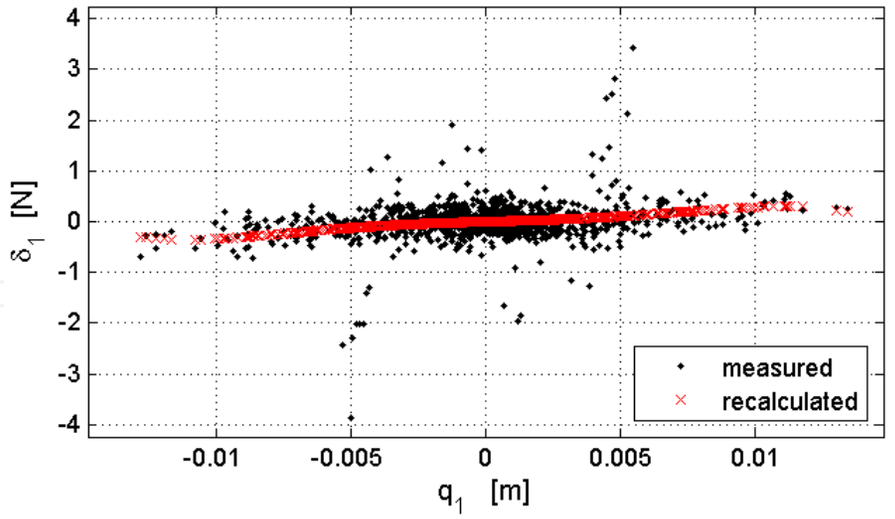

Figure 5. Non-linear restoring force of modal DoF 1 for single mode identification

case of *5 %* noise the deviations between the 'measured' and recalculated modal coordinates $q_1(t)$ and $q_3(t)$ amount to *7.4 %* and *7.7 %* respectively. It is apparent that no smaller deviation than *5 %* will be possible. Thus, the deviations are acceptable and indicate a good identification.

Figure 6 shows as an example the restoring force $\delta_1(q_1, q_3)$ identified from signals with *5 %* noise for mode $r = 1$. In the figure the 'measured' and recalculated restoring forces at all time steps are plotted as points and crosses. Also, the interpolated restoring surface is depicted. The interpolated restoring surface is computed at a grid of 25×10 data points. The grid is spanned between the minimum and maximum values of q_1 and q_3. The values of the restoring surface are obtained by using Eq. (42) with the identified coefficients α_{ij} and inserting the values at the grid points for q_1 and q_3. The figure shows clearly that the restoring force $\delta_1(q_1, q_3)$ depends on both modal coordinates. If modal coordinate q_3 would be set to zero (or any other fixed value), which is assumed during single mode identification, just a trim curve would be identified. However, this trim curve is not able to describe the complete non-linear behaviour.

6. Experimental example

In this section an example of the application of the method in practice is shown. The method is exemplarily applied to an aileron mode of a large transport aircraft (Goege, Fuellekrug, Sinapius, Link, & Gaul, 2005), (Goege & Fuellekrug, 2004) (Goege, 2004).

6.1. Test structure and test performance

A modal identification test is performed as a Ground Vibration Test on an aircraft using the modal identification concept described above. The test duration was about two weeks and the aircraft was tested in two configurations. A total number of 352 accelerometers was employed to measure the mode shapes of the structure with a sufficient spatial resolution.

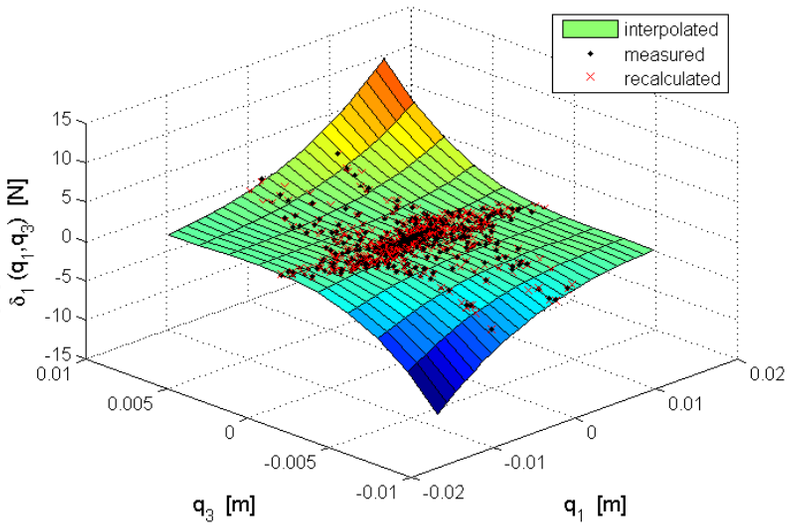

Figure 6. Restoring force of modal DoF 1 for coupled mode identification

The transport aircraft is dynamically characterized by a high modal density. During the GVT about 73 modes were identified. Most of the modes were linear. Only few modes exhibit non-linear behaviour. One mode with significant non-linear behaviour is the aileron mode.

6.2. Non-linear analysis

At first, the modal characteristics of the aileron mode were identified with the Phase Resonance Method at a level of the modal force of *10 N*. The aileron mode was excited with one single exciter, which was located at the aileron. Figure 7 displays schematically the test setup for the excitation of the aileron.

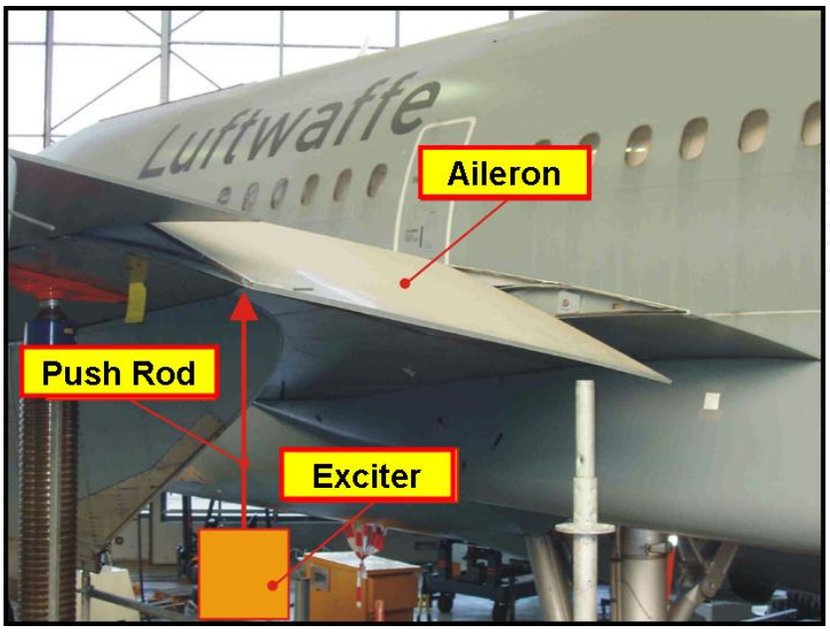

Figure 7. Excitation of the aileron mode of a large transport aircraft

Next, the level of the modal force was increased in several steps up to *121 N*. At each force level the aileron mode was measured with the Phase Resonance Method. Significant non-linear characteristics were observed: The resonance frequency of the aileron mode was changing over the load level by approximately *27 %*.

For the detailed non-linear analysis short parts of the time domain signals with harmonic steady-state excitation at the linear resonance frequency were measured. About 16 cycles of vibration were recorded. The modal accelerations were computed from the measured signals of the 352 accelerometers according to Eq. (35). The acceleration signals were filtered and integrated to obtain velocities and displacements as described above.

The analysis of the modal displacements was performed in the same way as for the simulated example. Figure 8 shows the RMS-values of the modal displacements for the lowest and highest excitation level. It shows that for the highest excitation level only the aileron mode $r = 60$ itself responds. However, for the lowest excitation level, a significant response of the bending mode of one winglet (mode $r = 71$) is also observed. This is not surprising because the motions of an aileron are in principle capable of exciting wing bending modes and thus motions of a winglet. The coupling of the aileron mode with all other modes is comparatively small.

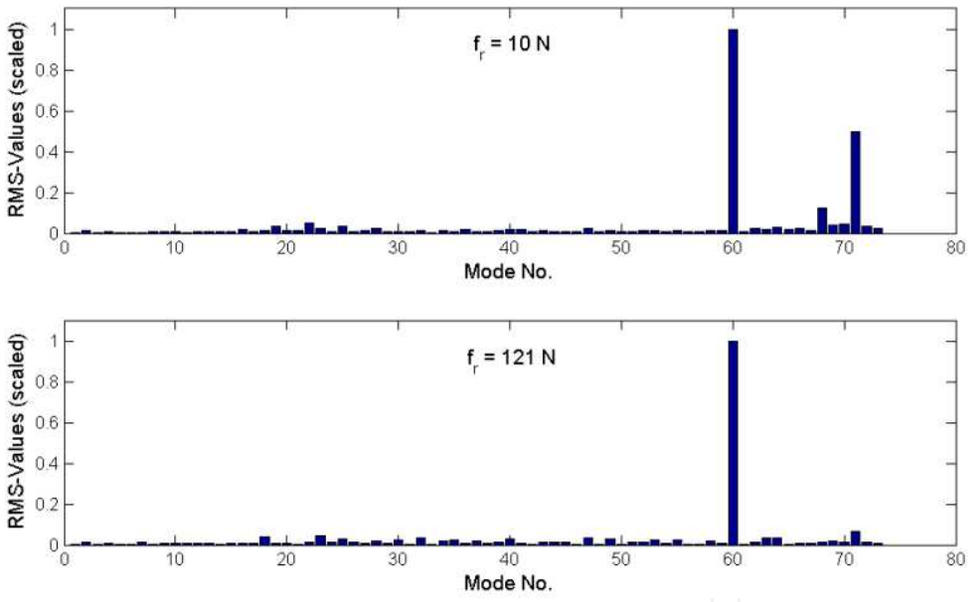

Figure 8. Mode participation for two different force levels

Figure 9 displays the restoring force of mode $r = 60$. The restoring force was calculated according to Eq. (34). In this equation the modal parameters, which were identified with the Phase Resonance Method on the highest level, are inserted together with the measured modal displacement q_{60} and the modal force f_{60}. The restoring function shows a hysteresis behaviour and may indicate a clearance non-linearity. This is imaginable because the structure vibrates at the lowest force level with only small amplitudes, which are close to the production tolerances of the aileron/wing attachment.

Under consideration of the observed mode coupling it makes sense to perform two types of non-linear identification: single mode identification for mode $r = 60$ and coupled mode identification for the two modes $r = 60$ and $r = 71$.

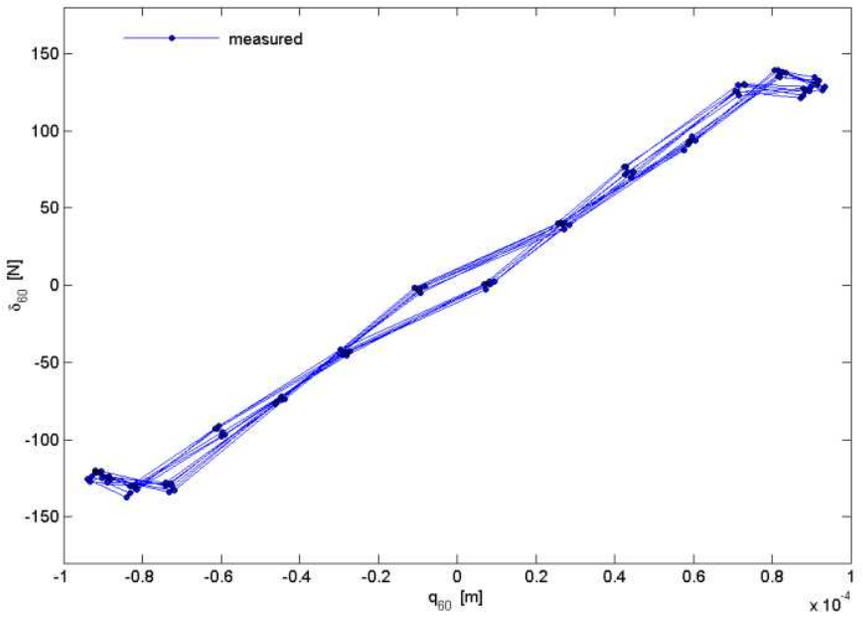

Figure 9. Measured restoring forces of the aileron mode

6.3. Single mode non-linear identification

For the single mode non-linear identification the polynomial functions of Eqs. (40) and (41) with the modal displacements and velocities of the aileron mode $r = 60$ are employed. The powers q_{60} and $\dot{q}_{60}$ are increased from $i_{\max} = 1$ to $i_{\max} = 3$. The selection of terms is performed in the way that several analysis runs with different terms on a trial and error basis are performed. The goal is to minimize the deviations between the measured and recalculated restoring forces and the measured and recalculated modal signals. Terms are included if they appear necessary to model the non-linear behaviour. They are excluded if they do not reduce the deviations. It turns out that the curve fit on the basis of Eqs. (40) and (41) is not completely successful. Thus, additional anti-symmetric terms on a trial and error basis are introduced. A stiffness term with the second power of q_{60}, namely $q_{60} \times \left|\dot{q}_{60}\right|$ reduces clearly the deviations and is therefore additionally included.

Table 1 shows the identified parameters which contribute clearly. The low value of the linear damping parameter γ_i constitutes only small changes with respect to the linear term, which is identified with the Phase Resonance Method and is a priori included in Eq. (34). No non-linear damping terms are detected.

Inserting the identified parameters in Eq. (37), the restoring force is calculated and displayed in Figure 10 together with the measured restoring force. It shows that the measured und recalculated restoring force match really well. Nevertheless, some deviations occur at the minima and maxima of the functions. The RMS-value of the deviation amounts to *0.90 %*.

Term of non-linearity	Single mode identification
q_{60}	$\alpha_1 = 3.204 \times 10^5$
$q_{60} \times \lvert q_{60} \rvert$	$\alpha_2 = 4.662 \times 10^{10}$
q_{60}^3	$\alpha_3 = -3.814 \times 10^{14}$
$\dot{q}_{60}$	$\gamma_1 = 7.0$

Table 1. Parameters for single mode identification

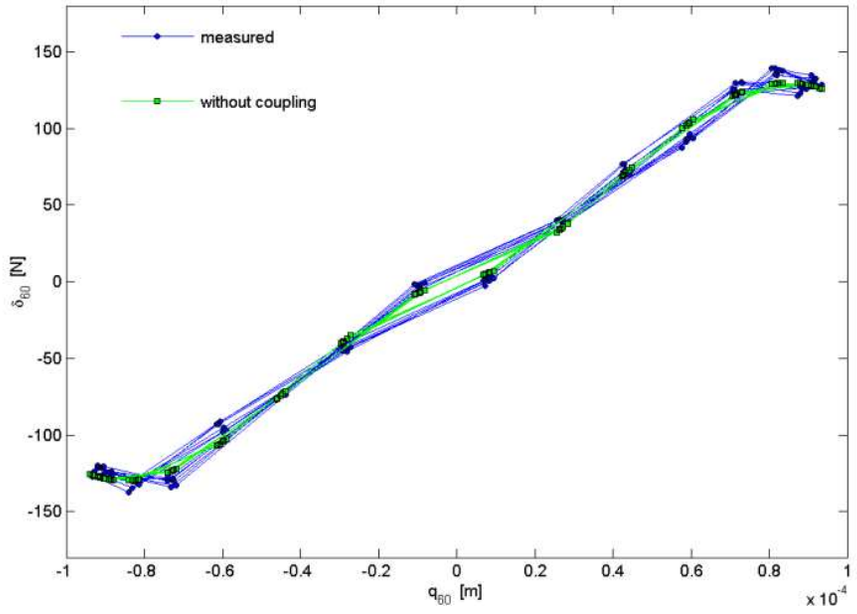

Figure 10. Measured and recalculated restoring forces (without coupling)

6.4. Coupled mode non-linear identification

For the coupled mode identification the polynomial functions of Eqs. (42) and (43) with the modal displacements and velocities of the aileron mode $r = 60$ and the winglet mode $r = 71$ are employed. The powers of q_{60}, q_{71} and $\dot{q}_{60}$, $\dot{q}_{71}$ are increased from $i_{\max} = j_{\max} = 1$ to $i_{\max} = j_{\max} = 3$. The selection of terms is performed in the same way as above. Several analysis runs with different terms on a trial and error basis are performed. Terms are only included if they contribute clearly to reduce the deviations between measured and recalculated modal signals.

Table 2 shows the identified parameters which contribute clearly. For mode $r = 60$ itself three stiffness and one damping parameter are identified again. In addition, two coupled stiffness and five coupled damping terms are identified. A significant difference to single mode identification for the four identified parameters of mode $r = 60$ is observed. The reason is that the analytical model has changed and that the coupled mode identification requires additional terms until the measured restoring forces are fitted with good accuracy. The different terms in the stiffness series compensate partly for each other. Thus, the physical meaning of the polynomial coefficients is limited. The polynomial coefficients may be considered rather as 'numbers' which enable a good fit to the measured data. The main criterion are the restoring functions.

Term of non-linearity	Coupled mode identification
q_{60}	$\alpha_1 = 2.264 \times 10^6$
$q_{60} \times \lvert q_{60} \rvert$	$\alpha_2 = -6.425 \times 10^9$
q_{60}^3	$\alpha_3 = -4.001 \times 10^{13}$
$\dot{q}_{60}$	$\gamma_1 = 1.190 \times 10^2$
$q_{60} \times q_{71}$	$\alpha_4 = 1.397 \times 10^9$
$q_{60}^2 \times q_{71}$	$\alpha_5 = 2.041 \times 10^{13}$
$\dot{q}_{60} \times \dot{q}_{71}$	$\gamma_2 = 1.806 \times 10^4$
$\dot{q}_{60}^2 \times \dot{q}_{71}$	$\gamma_3 = -1.458 \times 10^7$
$\dot{q}_{60} \times \dot{q}_{71}^2$	$\gamma_4 = -1.247 \times 10^6$
$\dot{q}_{60}^2 \times \dot{q}_{71}^3$	$\gamma_5 = 2.323 \times 10^{11}$
$\dot{q}_{60}^3 \times \dot{q}_{71}^3$	$\gamma_6 = -5.266 \times 10^{11}$

Table 2. Parameters for coupled mode identification

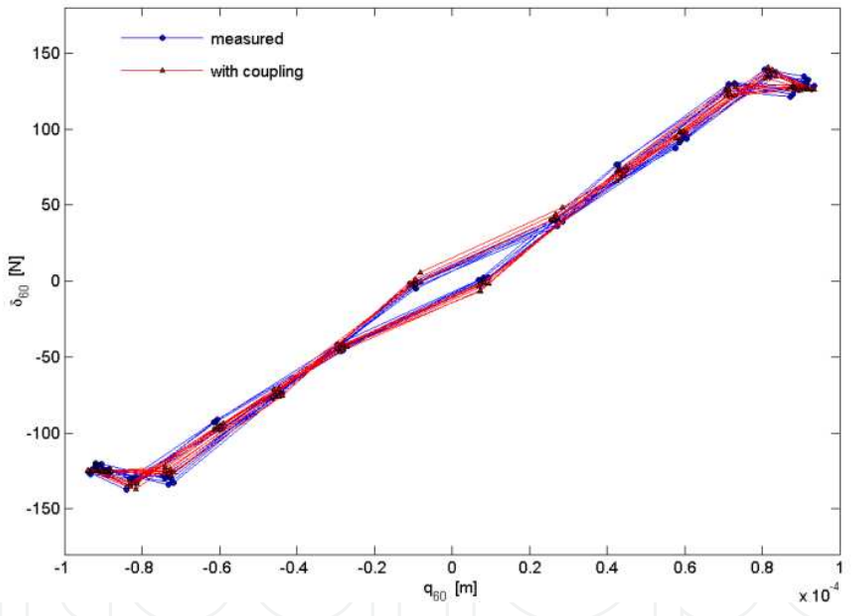

Figure 11. Measured and recalculated restoring forces (with coupling)

Figure 11 shows the measured and recalculated restoring forces. A nearly perfect agreement can be seen, even at the minima and maxima of the functions. The quantitative assessment via RMS-value delivers a deviation of *0.15 %*. In order to show the influence of the coupling terms, the restoring stiffness forces δ_{60} are visualized as surfaces in Figure 12.

The restoring surfaces are computed at a grid of data points which is spanned by the minimum and maximum values of q_{60} and q_{71}. The restoring force surface of the single mode nonlinear identification is computed at the grid points from Eq. (41) with the parameters of Table 1. This surface is depicted as black mesh. The restoring force surface of

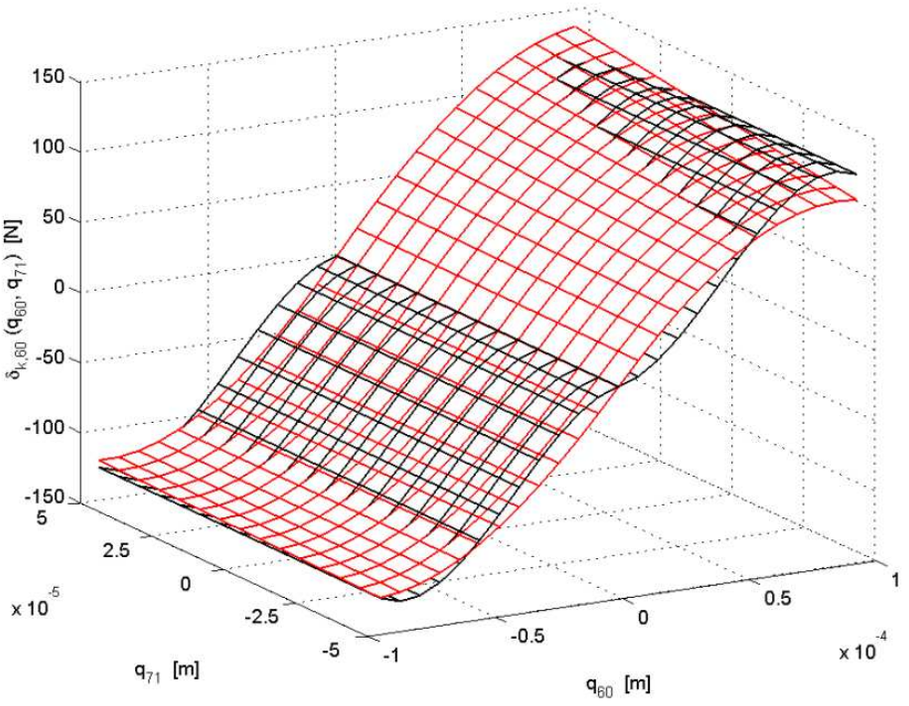

Figure 12. Restoring surface of single mode identification (black) and coupled mode identification (red)

the coupled mode identification is computed at the grid points from Eq. (42) with the parameters of Table 2. This surface is depicted as red mesh. Both surfaces exhibit a clear difference. Thus, the restoring force δ_{60} depends clearly from both modal coordinates q_{60} and q_{71}. Single mode identification with the black mesh restoring surface is not able to describe the complete non-linear behaviour.

7. Conclusion

This book chapter derives first the basic dynamic equations of structures with non-linearities and considers the experimental modal identification. Then the theoretical basis for non-linear identification is explained and a test strategy for non-linear modal identification, which can be used within a test concept for modal testing, is described. The basic idea is to use modal force appropriation, to employ equations in modal space and to identify the modal non-linear restoring forces. This is realized by computing the coefficients of applicable functions for the restoring forces from time domain data. The required steps for single mode and coupled mode non-linear identification are developed and discussed in detail. The identification is then illustrated by an analytical example where it could be shown that the method is able to identify the non-linear coupled modes of vibration. A second example taken from a modal identification test on a large transport aircraft shows the application of the approach in practice.

The non-linear identification may be further developed by using other functions for the restoring forces or to extend it to a higher number of modal DoF. Also, it can be elaborated whether and how it would be possible to derive the required linear modal parameters from

applying Phase Separation Techniques. Thus, the experimental effort of applying the Phase Resonance Method could be avoided leading to a reduced test duration.

Author details

Ulrich Fuellekrug
Institute of Aeroelasticity, Deutsches Zentrum fuer Luft- und Raumfahrt (DLR), Germany

8. References

Al_Hadid, M. A., & Wright, J. R. (1989, Vol. 3, No. 3). Developments in the Force-State Mapping Technique for Non-Linear Systems and the Extension to the Localisation of Non-Linear Elements in a Lumped Parameter System. *Mechanical Systems and Signal Processing*, pp. 269-290.

Awrejcewicz, J., & Krysko, V. A. (2008). *Chaos in Structural Mechanics.* Berlin: Springer-Verlag.

Awrejcewicz, J., Krysko, V. A., Papkova, I. V., & Krysko, A. V. (2012, 45). Routes to chaos in continuous mechanical systems. Part 1: Mathematical models and solution methods. *Chaos Solitons & Fractals*, pp. 687-708.

Awrejcewicz, J., Krysko, V. A., Papkova, I. V., & Krysko, A. V. (2012, 25). Routes to chaos in continuous mechanical systems. Part 3: The Lyapunov exponents, hyper, hyper-hyper and spatial-temporal chaos. *Chaos Solitons & Fractals*, pp. 721-736.

Crawley, E. F., & Aubert, A. C. (1986, Vol. 24, No. 1). Identification o f Nonlinear Structural Elements by Force-State Mapping. *AIAA Journal*, pp. 155-162.

Ewins, D. J. (2000). *Modal Testing: Theory, Practice and Application.* Baldock, Hertfordshire, England: Research Studies Press Ltd.

Fuellekrug, U. (1988, Vol. 27-1). Survey of Parameter Estimation Methods in Experimental Modal Analysis. *Journal of the Society of Environmental Engineers*, pp. 33-44.

Gloth, G., & Goege, D. (2004). Handling of Non-Linear Structural Characteristics in Ground Vibration Testing. *Proceedings of the International Conference on Noise and Vibration Engineering (ISMA)*, (pp. 2129-2143). Leuven (Belgium).

Gloth, G., Degener, M., Fuellekrug, U., Gschwilm, J., Sinapius, M., Fargette, P., & Levadoux, B. (2001, Vol. 35, No. 11). New Ground Vibration Testing Techniques for Large Aircraft. *Sound and Vibration*, pp. 14-18.

Goege, D. (2004). *Schnelle Identifikation und Charaktersisierung von Linearitaetsabweichungen in der experimentellen Modalanalyse grosser Luft- und Raumfahrtstrukturen.* Forschungsbericht DLR_FB_2004-36.

Goege, D., & Fuellekrug, U. (2004). Analyse von nichtlinearem Schwingungsverhalten bei großen Luft- und Raumfahrtstrukturen. *VDI Schwingungstagung, VDI-Berichte Nr. 1825*, (pp. 123-155). Wiesloch (Germany).

Goege, D., Fuellekrug, U., Sinapius, M., Link, M., & Gaul, L. (2005, Vol. 46, No. 5). INTL - A Strategy for the Identification and Characterization of Non-Linearities within Modal Survey Testing. *AIAA Journal*, pp. 974-986.

Goege, D., Sinapius, M., Fuellekrug, U., & Link, M. (2005, Vol. 40). Detection and Description of Non-Linear Phenomena in Experimental Modal Analysis Via Linearity Plots. *International Journal of Non-Linear Mechanics*, pp. 27-48.

Krysko, V. A., Awrejcewicz, J., Papkova, I. V., & Krysko, A. V. (2012, 45). Routes to chaos in continuous mechanical systems. Part 2: Modelling transitions from regular to chaotic dynamics. *Chaos Solitons & Fractals*, pp. 709-720.

Landau, L. D., & Lifschitz, E. M. (1976). *Lehrbuch der theoretischen Physik - Mechanik.* Akademie Verlag.

Maia, N. M., & Silva, J. M. (1997). *Theoretical and Experimental Modal Analysis.* New York: John Wiley & Sons Inc.

Masri, S. F., & Caughey, T. K. (1979, Vol. 46). A Nonparametric Identification Technique for Nonlinear Dynamic Systems. *Journal of Applied Mechanics*, pp. 433-447.

Niedbal, N., & Klusowski, E. (1989, Vol. 13, No. 3). Die Ermittlung der generalisierten Masse und des globalen Daempfungsbeiwertes im Standschwingungsversuch. *Zeitschrift für Flugwissenschaften und Weltraumforschung*, pp. 91-100.

Platten, M. F., Wright, J. R., Cooper, J. E., & Sarmast, M. (2002). Identifcation of Multi-Degree of Freedom Non-Linear Simulated and Experimental Systems. *Proceedings of the International Conference on Noise and Vibration Engineering (ISMA*, (pp. 1195-1202). Leuven (Belgium).

Platten, M., Wrigth, J., Dimitriadis, G., & Cooper, J. (2009, Vol. 23, No. 1). Identification of multi degree of freedom non-linear systems using an extended modal space model. *Mechanical Systems and Signal Processing*, pp. 8-29.

Platten, M., Wrigth, J., Worden, K., Cooper, J., & Dimitriadis, G. (2005). Non-Linear Identification Using a Genetic Algorithm Approach for Model Selection. *Proceedings of the 23rd International Modal Analysis Conference (IMAC-XXIII).* Orlando, FL (USA).

Szabo, I. (1956). *Höhere Technische Mechanik.* Berlin/Göttingen/Heidelberg: Springer Verlag.

Williams, J. H. (1996). *Fundamentals of Applied Dynamics.* New York: John Wiley & Sons, Inc.

Worden, K., & Tomlinson, G. R. (2001). *Nonlinearity in Structural Dynamics -Detection, Identification and Modelling-.* Bristol and Philadelphia: Insitute of Physics Publishing.

Wright, J., Platten, M., Cooper, J., & Sarmast, M. (2001). Identification of Multi-Degree of Freedom Weakly Non-linear Systems using a Model based in Modal Space. *Proceedings of the International Conference on Strucutral System Identification*, (pp. 49-68). Kassel (Germany).

Wrigth, J., Platten, M., Cooper, J., & Sarmast, M. (2003). Experimental Identification of Continuous Non-Linear Systems Using an Extension of Force Appropriation. *Proceedings of the 21st International Modal Analysis Conference (IMAC-XXI).* Kissimmee, FL (USA).

IntechOpen